Article:
Sampson, J, O'Regan, L, Dyer, MJS et al. (2 more authors) (2017) Hsp72 and Nek6 cooperate to cluster amplified centrosomes in cancer cells. Cancer Research, 77 (18). pp. 4785-4796. ISSN 0008-5472

https://doi.org/10.1158/0008-5472.CAN-16-3233

Hsp72 and Nek6 cooperate to cluster amplified centrosomes in cancer cells

Josephina Sampson[1], Laura O'Regan[1], Martin J.S. Dyer[2], Richard Bayliss[3] and Andrew M. Fry[1]

[1]Department of Molecular and Cell Biology, and [2]Ernest and Helen Scott Haematological Research Institute, University of Leicester, Lancaster Road, Leicester LE1 9HN, U.K.

[3]Astbury Centre for Structural Molecular Biology, Faculty of Biological Sciences, University of Leeds, Leeds LS2 9JT, U.K.

Running Title: Hsp72 and Nek6 promote centrosome clustering in cancer cells

Keywords: centrosome, mitosis, Hsp72, Nek6, griseofulvin, acute lymphoblastic leukaemia

Financial Support:

This work was funded by grants from Hope Against Cancer (PHD/SELLICKS/BLN/2013), the Medical Research Council (MR/J003972/1), Worldwide Cancer Research (16-0119), The Wellcome Trust (097828/Z/11/Z) and Cancer Research UK (C1362/A18081) to A.M. Fry, and grants from Cancer Research UK (C24461/A23303) and BBSRC (BB/L023113/1) to R. Bayliss.

Correspondence should be addressed to:

Andrew M. Fry, Department of Molecular and Cell Biology, University of Leicester, Lancaster Road, Leicester LE1 9HN, U.K.

Email: amf5@le.ac.uk; Tel: +44 116 229 7069; Fax: +44 116 229 7018

Conflict of Interest Statement:

The authors declare no conflicts of interest.

ABSTRACT

Cancer cells frequently possess extra amplified centrosomes clustered into two poles whose pseudo-bipolar spindles exhibit reduced fidelity of chromosome segregation and promote genetic instability. Inhibition of centrosome clustering triggers multipolar spindle formation and mitotic catastrophe, offering an attractive therapeutic approach to selectively kill cells with amplified centrosomes. However, mechanisms of centrosome clustering remain poorly understood. Here, we identify a new pathway that acts through NIMA-related kinase 6 (Nek6) and Hsp72 to promote centrosome clustering. Nek6, as well as its upstream activators polo-like kinase 1 (Plk1) and Aurora-A, targeted Hsp72 to the poles of cells with amplified centrosomes. Unlike some centrosome de-clustering agents, blocking Hsp72 or Nek6 function did not induce formation of acentrosomal poles, meaning that multipolar spindles were observable only in cells with amplified centrosomes. Inhibition of Hsp72 in acute lymphoblastic leukaemia cells resulted in increased multipolar spindle frequency that correlated with centrosome amplification, while loss of Hsp72 or Nek6 function in non-cancer derived cells disturb neither spindle formation nor mitotic progression. Hence, the Nek6-Hsp72 module represents a novel actionable pathway for selective targeting of cancer cells with amplified centrosomes.

INTRODUCTION

The mitotic spindle is bipolar in nature as it is organised around two poles, each possessing a single centrosome (1,2). However, the majority of cancer cells have extra or 'amplified' centrosomes that would be expected to form multipolar spindles leading to mitotic catastrophe and cell death (3,4). Cancer cells solve this problem by either inactivating the extra centrosomes or clustering them into two poles to form a pseudo-bipolar spindle (5). The added time taken to organize such a spindle and presence of more than two centrosomes in early mitosis favours generation of merotelic microtubule-chromosome attachments that are poorly recognized by the spindle assembly checkpoint (SAC) (6,7). Hence, amplified centrosomes are not only tolerated but promote chromosome segregation errors, genome instability and cancer progression (8-10).

Centrosomes act as the dominant microtubule organizing centres (MTOCs) in proliferating animal cells because they recruit the γ-tubulin ring complex (γ-TuRC) from which microtubules are nucleated (11,12). The γ-TuRC is concentrated at centrosomes through binding to components of the pericentriolar material (PCM), a highly ordered matrix of coiled-coil proteins that surrounds and is scaffolded by a pair of centrioles (13). The centrioles are composed of nine triplets of highly stable microtubules organised into a polarised barrel that is duplicated once per cell cycle. Hence, cells in G1 have two centrioles, while cells in late G2 have four centrioles (14). These centrioles remain in close proximity during interphase due to proteinaceous ties that link them together (15). While each centriole is associated with its own PCM, the close juxtaposition of new centrioles with their parental centrioles in S/G2 mean that only two distinct PCM clouds are visible both before and after duplication. Hence, when scoring centrosome amplification, we use the criteria that cells should have more than two PCM foci and more than four centrioles.

Experimental studies have revealed a number of microtubule-based processes that promote centrosome clustering, including motor protein activity, microtubule dynamics, and microtubule attachments to the centrosome, chromosomes and cell cortex (16-18). In addition, the extra time taken to organize a pseudo-bipolar spindle in cells with amplified centrosomes means that

clustering requires cells to have a robust spindle assembly checkpoint (SAC) that can delay anaphase onset until complete chromosome congression has been achieved (16,19). Targeting these different clustering processes could provide a selective approach to killing cancer cells with amplified centrosomes (20). However, the underlying mechanisms remain far from understood.

Uncoupling of the centrosome duplication cycle from the cell cycle can result from altered activity of tumour suppressor genes and oncogenes and is a major route to centrosome amplification in cancer cells (21-23). This could arise from changes in gene expression of centrosome duplication regulators caused by deregulated signal transduction pathways. Alternatively, it could be due to reduced integrity of checkpoints, such as the SAC or DNA damage checkpoints, which disturb the timing of cell cycle progression and perturb coordination with the centrosome duplication cycle. Cancer cells also need to tolerate the presence of amplified centrosomes and destabilization of p53 through inactivation of the Hippo pathway may be a common mechanism in this regard (24).

Oncogenesis is associated with proteotoxic stress that leads to induction of heat shock proteins (HSPs) required to maintain protein folding and homeostasis (25,26). As such HSPs represent cancer targets that are not necessarily restricted to tumours with particular driver mutations (27,28). Using RNAi depletion and chemical inhibitors, we recently found that Hsp72 is essential for mitotic spindle assembly in cancer cells, promoting stabilization of kinetochore-associated microtubules, (K)-fibres, through recruitment of the chTOG-TACC3 complex (29). This function of Hsp72 is dependent upon its phosphorylation by the Nek6 mitotic kinase. As Hsp72 and Nek6 are required for K-fibre stability and robust mitotic spindle assembly, we reasoned that they might also be required for clustering of amplified centrosomes. Here, we set out to test this hypothesis using fixed and time-lapse imaging of MDA-MB-231 (human breast carcinoma) and NIE-115 (mouse neuroblastoma) cell lines that harbor amplified centrosomes and exhibit centrosome clustering activity (16,30,31). Our data reveal a new pathway of centrosome clustering and lead us to propose a therapeutic role for Hsp72 and/or Nek6 inhibitors as selective de-clustering agents in cancer cells with amplified centrosomes.

MATERIALS AND METHODS

Cell culture, synchronisation, transfection and drug treatments

All media were from Invitrogen and supplemented with 10% heat-inactivated foetal bovine serum (FBS), 100 IU/ml penicillin and 100 mg/ml streptomycin. MDA-MB-231, HeLa and HBL-100 cells were obtained from Cell Lines Service (CLS), while NIE-115 and RPE1-hTERT cells were obtained from ATCC. MDA-MB-231, NIE-115, HeLa and HBL-100 cells were cultured in Dulbecco's modified Eagle's medium (DMEM), while RPE1-hTERT cells were grown in DMEM-F12 with 0.25% sodium bicarbonate. Acute lymphoblastic leukemic (ALL) cells were obtained from the Leibniz Institute DSMZ-German Collection of Microorganisms and Cell Cultures (http://www.celllines.de) and grown in RPMI 1640 medium. PBLs are EBV transformed B-cells obtained from the Coriell Institute for Medical Research Biorepository (https://catalog.coriell.org). All cells were obtained within the last 10 years, stored in liquid nitrogen, and maintained in culture at 37°C in a 5% CO_2 atmosphere for a maximum of 2 months. We relied on the provenance of the original collections for authenticity, while mycoplasma infection was avoided through bimonthly tests using an in-house PCR-based assay. RNAi-resistant wild-type and kinase-dead (KD, K75M) Flag-Nek6 constructs were generated using the QuikChange Site-Directed Mutagenesis Kit (Agilent Technologies) and transfections performed with Lipofectamine 2000 reagent (Life Technologies) according to manufacturers' instructions. Unless otherwise indicated, the following inhibitors were added to cells for 4 h: VER-155008 (Hsp70i, 10 µM; Tocris Bioscience); Griseofulvin (10 µM; Sigma); MLN8054 (Aurora-Ai; 500 nM; MedChem Express); BI-2536 (Plk1i; 100 nM; MedChem Express). Control cells were treated with the same volume of DMSO. For microtubule regrowth, cells were incubated for 16 h with 50 ng/ml nocodazole (Sigma) followed by treatment with the 10 µM VER-155008 for 2 h. M-phase arrested cells were prepared by mitotic shake-off after 16 h nocodazole treatment.

Fixed and live cell microscopy

Adherent cells were grown on acid-etched glass coverslips while suspension cells were seeded onto Superfrost Plus glass slides (Thermo). Cells were fixed with ice-cold methanol before being processed for immunofluorescence microscopy as previously described (29,32,33). For Hsp72 staining, cells were incubated for 30 seconds in pre-extraction buffer (60 mM Pipes, 25 mM Hepes, pH7.4, 10 mM EGTA, 2 mM $MgCl_2$, and 1% Triton X-100) prior to fixation. Primary antibodies were against α-tubulin (0.3 µg/ml; Sigma), γ-tubulin (0.5 µg/ml; Sigma), centrin-2 (N-17) (0.4 µg/ml; Santa Cruz Biotechnology), CEP135 (2 µg/ml; OriGene), pericentrin (2 µg/ml; Abcam), CenpA (2 µg/ml; Abcam), Hsp72 (0.8 µg/ml; C92F3A-5; Enzo Life Sciences), BubR1 (10 µg/ml; Abcam) and phospho-Histone H3 (2 µg/ml; Abcam). DNA was stained with 0.8 µg/ml Hoechst 33258. Secondary antibodies were Alexa Fluor-488 and -594 goat anti-rabbit and goat anti-mouse IgGs (1 µg/ml; Invitrogen). Imaging was performed on a Leica TCS SP5 confocal microscope equipped with a Leica DMI 6000B inverted microscope using a 63x oil objective (numerical aperture, 1.4). Z-stacks comprising of 30-50 x 0.3 µm sections were acquired. Time-lapse imaging was performed on a Leica TCS SP5 confocal microscope equipped with a Leica DMI 6000B inverted microscope using a 63x oil objective (numerical aperture, 1.4). Cells were cultured in glass-bottomed culture dishes (MatTek Corp.) and maintained at 37℃ in an atmosphere supplemented with CO_2 using a microscope stage temperature control system (Life Imaging Services). 50 nM SiR-tubulin (Spirochrome; SC002) was added 7 h before imaging when required. Z-stacks comprising 20 x 0.5 µm sections were acquired every 5 min for a minimum of 16 h. Stacks were processed as maximum intensity projections using LAS-AF software (Leica) and movies prepared using ImageJ (v.1.51). To quantify spindle association of Hsp72, the mean pixel intensity over the whole spindle was measured using Volocity software and normalized to spindle microtubule intensity, while BubR1 association with kinetochores was quantified by measuring total pixel intensity over the chromatin using ImageJ software.

RNAi

Cells were seeded at 30-40% confluency in Opti-MEM Reduced Serum Medium and transfected using Oligofectamine (Life Technologies, UK) according to manufacturer's instructions. 100 nM

ON-TARGETplus siRNA duplexes were used against human Hsp72 (J-005168-06, J-005168-07), Nek6 (J-004166-06, J-004166-09) or Nek7 (J-003795-12, J-003795-14), or mouse Hsp72 (J-054644-05, J-054644-07) obtained from Thermo Fisher Scientific (Lafayette, CO), or GAPDH (4390850), obtained from Life Technologies. siRNA duplexes were transfected. Cells were prepared for microscopy or Western blot analysis 72 h after transfection of siRNA duplexes.

Cell lysis, SDS-PAGE and Western blotting

Preparation of cell lysates, SDS-PAGE and Western blotting were performed as previously described (34). For Western blotting, primary antibodies were against Nek6 (1 µg/ml, Abcam), Nek7 (0.5 µg/ml, Abcam), Hsp72 (0.5 µg/ml, Enzo Life Sciences), Hsc70 (1 µg/ml, Santa Cruz) and GAPDH (1:1000, Cell Signaling). Secondary antibodies were goat or donkey anti-rabbit and anti-mouse horseradish peroxidase (HRP)-labelled IgGs (1:1000; Amersham, U.K.).

Statistical analysis

All quantitative data represent means and SD of at least three independent experiments. Statistical analyses were performed using a one-way ANOVA analysis; ****$p<0.0001$, ***$p<0.001$, **$p<0.01$, *$p<0.05$.

RESULTS

Hsp72 is required for centrosome clustering in cancer cells

To examine the role of Hsp72 in centrosome clustering, we first assessed the frequency of centrosome amplification in a set of cancer and non-cancer-derived cell lines using antibodies against γ-tubulin to count PCM foci and centrin-2 to score centrioles (Fig. 1A). Consistent with previous studies (16,30,31), 33.5% MDA-MB-231 human breast cancer and 96% NIE-115 mouse neuroblastoma cells were found to have >2 centrosomes in interphase, whereas only 8.3% HeLa human cervical cancer and 1% human RPE1 (retinal pigment epithelial cells immortalised with hTERT) had >2 centrosomes (Fig. 1B). To assess spindle polarity, cells were stained with antibodies against α-tubulin to detect microtubules and centrin-2 to score centrosomes. Scoring

only mitotic cells with >2 centrosomes (i.e. >4 centrin-2 stained centrioles), 82% MDA-MB-231 and 76% NIE-115 cells formed pseudo-bipolar spindles with the amplified centrosomes clustered at two poles (Fig. 1C, D).

Spindle organization was then assessed in MDA-MB-231 and NIE-115 cells treated with increasing doses (5-20 μM) VER-155008, a chemical inhibitor of Hsp70 (35). This revealed a dose-dependent increase in the frequency of cells with amplified centrosomes that had multipolar spindles following treatment with the Hsp70i (Fig. 1E-G). As VER-155008 inhibits all members of the Hsp70 family, we confirmed the specific role of the inducible Hsp72 isoform in centrosome clustering using two independent siRNA oligonucleotides to deplete the protein from MDA-MB-231 and NIE-115 cells. Both siRNAs caused a significant increase in multipolar spindles in cells with amplified centrosomes as compared to mock-depleted cells, while Western blotting confirmed that siRNAs depleted Hsp72 but not the constitutive Hsc70 in each cell line (Fig. 1H, I, and Supp. Fig. S1A, B). Hence, we conclude that Hsp72 is essential for centrosome clustering in cancer cells with amplified centrosomes.

Hsp72 promotes resolution of multipolar to bipolar spindles

To analyse the role of Hsp72 in centrosome clustering, we took advantage of a far-red fluorescent probe, SiR-tubulin, that can stain microtubules in live cells (33,36). Addition of SiR-tubulin revealed the initial assembly of multipolar spindles in NIE-115 cells following mitotic entry (Fig. 2A, B). However, following a mean time of 78 mins in a multipolar state, these spindles subsequently resolved into a bipolar state before cells progressed into anaphase and completed division (Fig. 2C). In the presence of the Hsp70i, there was little difference from untreated cells in the length of prophase, measured from when a robust microtubule array formed to when nuclear envelope breakdown occurred. However, after assembling a multipolar spindle, this state was maintained for extended time in the presence of the Hsp70i with only ~50% cells resolving the spindle into a pseudo-bipolar state within the time-frame of the experiment (700 mins); for those cells in which the spindle did resolve into a pseudo-bipolar state they spent a mean of 480 mins in

metaphase (Fig. 2A-C). Analysis of cells depleted of Hsp72 using the same approach gave similar results confirming the specific role of Hsp72 in this process (Fig. 2C). Likewise, inhibition of Hsp70 or depletion of Hsp72 in MDA-MB-231 cells led to multipolarity with a mean time of >500 mins in metaphase (Fig. 2D). These data reveal that in these cell types the multiple MTOCs generated by the presence of amplified centrosomes are resolved to a pseudo-bipolar state as a result of centrosome clustering rather than centrosome inactivation. Moreover, they confirm that loss of Hsp72 function prevents this from occurring thereby stopping cells from satisfying the SAC and proceeding into late mitosis.

Nek6 kinase activity is required for centrosome clustering in cancer cells

Our previous studies revealed that Hsp72 promotes spindle assembly in mitotic cells downstream of the protein kinase Nek6 (29). To determine whether a similar pathway is involved in centrosome clustering, we depleted MDA-MB-231 cells of either Nek6 or the closely related Nek7 kinase. Although Nek6 and Nek7 have almost identical catalytic sites, they have distinct substrate specificities that result from their distinct N-termini (37), and Nek6 but not Nek7 interacts with Hsp72 (29). Each kinase was independently depleted with two different oligonucleotides and depletion confirmed by Western blot (Supp. Fig. S1C). Whereas removal of Nek7 had no effect on centrosome clustering, depletion of Nek6 led to a substantial increase in the frequency of cells with amplified centrosomes that had multipolar spindles indicative of a failure in centrosome clustering (Fig. 3A, B). Strikingly, wild-type but not kinase-inactive Nek6 was capable of rescuing centrosome clustering in cells from which Nek6 had been depleted demonstrating the requirement for Nek6 kinase activity in this process (Fig. 3B).

In MDA-MB-231 cells that had been detergent-extracted prior to fixation to remove soluble protein, Hsp72 was observed at spindle poles consistent with previous observations in other cell types (29,38-40). However, this localization was lost upon Nek6, but not Nek7, depletion despite no change in overall expression of Hsp72 (Fig. 3C, D; Supp. Fig. S1D). Further evidence that Nek6 and Hsp72 cooperate in centrosome clustering came from demonstrating that chemical

inhibition of either Aurora-A or Plk1, both of which act upstream of Nek6 and induce monopolar spindle formation (41,42), prevent localization of Hsp72 to spindle poles without disturbing its expression (Fig. 3C, D, and Supp. Fig. S1E, F). Similar loss of Hsp72 localization upon Aurora-A or Plk1 inhibition was observed in NIE-115 cells (Fig. 3E). Thus, we propose that a pathway acting through the Aurora-A, Plk1 and Nek6 kinases targets Hsp72 to the spindle apparatus.

Mitotic cells lacking Hsp72 or Nek6 activity do not form acentrosomal spindle poles

As a potential strategy for targeting cancer cells with amplified centrosomes, we compared the phenotypes generated upon loss of Hsp72 or Nek6 function, with the action of a well characterised centrosome declustering agent, griseofulvin (43). As expected, griseofulvin induced generation of multipolar spindles in MDA-MB-231 cells with amplified centrosomes (Fig. 4A, B). However, it led to an even higher frequency of multipolar spindles in HeLa cells, which do not exhibit substantial centrosome amplification (Fig. 4A, B). Analysis of these cells with centriole markers revealed that griseofulvin induces formation of microtubule asters in mitotic cells that lack centrioles, so called ‘acentrosomal’ poles (Fig. 4C, D). In contrast, MDA-MB-231 cells treated with the Hsp70i, or depleted of Hsp72 or Nek6, did not form acentrosomal poles, with all poles in the multipolar spindles containing centrioles (Fig. 4C, D).

Acentrosomal poles also arise in mitotic cells following nocodazole-induced microtubule depolymerisation and subsequent nocodazole washout. However, these quickly resolve to form a bipolar spindle. To observe, how cells with acentrosomal poles respond in the absence of Hsp70 activity, NIE-115, MDA-MB-231 and HeLa cells were treated for 16 h with nocodazole and then released into nocodazole-free media in the presence or absence of the Hsp70i (Supp. Fig. S2A). In the absence of Hsp70i, NIE-115 cells initially had multiple microtubule asters but these largely resolved within 60 mins to two asters (Fig. 4E, and Supp. Fig. S2B). However, in the presence of the Hsp70i, these multiple asters did not resolve and the percentage of cells with >2 asters remained relatively constant. With the MDA-MB-231 cells, there was a partial resolution in the presence of the Hsp70i consistent with the lower frequency (~35%) of cells with amplified

centrosomes (Fig. 4F). In contrast, in HeLa cells that do not have amplified centrosomes, the multiple asters resolved to form a bipolar spindle at a similar rate in the presence or absence of Hsp70i (Fig. 4G, and Supp. Fig. S2C). Hence, Hsp70 is required to cluster microtubule asters organised by bona fide centrosomes, but not to cluster microtubule asters generated by acentrosomal poles.

Spindle polarity correlates with centrosome number in ALL cells

To address the role of inhibiting Hsp70 in a particular cancer setting, we opted to assess a panel of acute lymphoblastic leukaemia (ALL) cell lines, on the basis that childhood ALL is a cancer typically treated with the microtubule poison, vincristine (44). This treatment is effective but associated with significant toxicity and risks of secondary cancers due to the lack of selectivity for cancer cells. For this analysis, ten ALL cell lines were analysed as well as two non-cancer derived peripheral B-lymphocyte (PBL) cell lines. Despite being non-adherent cell lines with high nuclear-to-cytoplasmic ratios that make them sub-optimal for imaging, we optimised techniques to assess centrosome number using antibodies against Cep135 to stain centrioles and either γ-tubulin or pericentrin to stain the PCM (33). While PBLs had a very low frequency (<5%) of cells with amplified centrosomes, the majority of ALL cell lines exhibited centrosome amplification within a range of 10-30% cells (Fig. 5A, B). Treatment with the Hsp70i revealed a dose-dependent increase in the frequency of multipolar spindles that correlated strongly with extent of centrosome amplification (Fig. 5C, D). In contrast, griseofulvin induced multipolar spindle formation to the same extent in all cells, including the PBLs, due to generation of acentrosomal poles (Fig. 5E, F). Western blotting revealed increased expression of Hsp72 in most, but not all ALL cell lines compared to PBLs, while Nek6 was present at similar levels in ALL and PBL cell lines (Supp. Fig. S1F). Hence, inhibiting the Nek6-Hsp72 pathway represents a potential route to selective targeting of ALL cells with amplified centrosomes.

Hsp72 and Nek6 are not required for mitotic progression in non-cancer derived cells

Targeting the Nek6-Hsp72 pathway for cancer therapy would only improve selectivity if these proteins are not required for proliferation of normal cells. In fact, we have previously shown that this pathway is required for robust spindle assembly in HeLa cells arguing that their role extends beyond centrosome clustering in cancer cells (29). Importantly, we found that while Hsp70 inhibition blocked chromosome congression in both HeLa and MDA-MB-231 cells, treatment with the Hsp70i did not lead to chromosome congression defects in the non-cancer derived RPE1 and HBL-100 cell lines (Fig. 6A, B). Encouragingly, we also found that depletion of Hsp72 or Nek6 led to a similar level of chromosome congression defects in HeLa and MDA-MB-231 cells, but did not interfere with chromosome congression in RPE1 and HBL-100 cells (Fig. 6C). Measurement of mitotic index by analysis of condensed chromatin and staining for the phospho-histone H3 (pHH3) marker confirmed that Hsp70 inhibition caused a significant delay in mitotic progression in HeLa and MDA-MB-231 cells, but not in RPE1 and HBL-100 cells (Fig. 6D, and Supp. Fig. S3A). Time-lapse imaging of RPE1 cells incubated with the SiR-tubulin probe also revealed no change in mitotic duration or spindle shape upon treatment with the Hsp70i or depletion of Hsp72 (Fig. 6E, and Supp. Fig. S3B, C). As expected, Western blotting revealed that the non-cancer derived cells lines, RPE1 and HBL-100, exhibited lower expression levels of the inducible Hsp72 protein than the cancer lines, MDA-MB-231 and HeLa (Supp. Fig. S3D, E). Finally, we showed that while Hsp70 inhibition can perturb K-fibre assembly, it did not prevent SAC activation as determined by recruitment of BubR1 in nocodazole-treated MDA-MB-231 cells (Fig. 6F, G). Thus, we propose that the Nek6-Hsp72 pathway is required for spindle organization and centrosome clustering, but not SAC activity, in cancer cells but not essential for mitotic progression in normal cells. This pathway therefore represents an attractive target for development of novel anti-cancer therapies.

DISCUSSION

Centrosome amplification is frequently observed in cancer cells and associated with poor prognosis (3). To allow cell survival, the extra centrosomes are clustered to enable formation of a pseudo-bipolar spindle that can support chromosome segregation. Centrosome clustering has

therefore emerged as a potentially exciting avenue for cancer drug discovery based on the principle of selective disruption of mitosis in cells with amplified centrosomes (18,45).

Here, we demonstrate that the Nek6-Hsp72 axis, together with the upstream Aurora-A, Plk1 and presumably Nek9 kinases, represents a novel pathway for regulating centrosome clustering (Fig. 6H). Nek6-phosphorylated Hsp72 regulates the spindle association of the chTOG-TACC3 complex (29). This complex was previously implicated in centrosome clustering through its regulation by integrin-linked kinase (ILK), inhibition of which prevents centrosome clustering (30). Spindle association of chTOG-TACC3 also requires clathrin, a known binding partner of Hsp70 chaperones (46). Our working hypothesis is that phosphorylation of Hsp72 by Nek6 modulates the interaction of clathrin with TACC3 and/or microtubules to favour spindle association of the complex, thereby promoting K-fibre stability (47). However, there could equally be other Nek6 and/or Hsp72 targets associated with centrosome and/or kinetochore attachments (including motors, such as Eg5, HSET or dynein) that promote tension in K-fibres. These mechanisms are under investigation.

A major challenge is to identify mechanisms that play an essential role in centrosome clustering but which can be safely inhibited in normal cells. Multipolar spindles can result from perturbation of many different spindle associated proteins, but there are few examples so far of proteins that show selective effects in cancer cells with amplified centrosomes and that are amenable to inhibition with a drug-like molecule. One example is HSET/KIFC1, a minus end-directed microtubule motor of the kinesin-14 family (48,49). Multipolar spindle formation is induced upon treatment of cancer cells harbouring amplified centrosomes with either of two distinct HSET inhibitors: AZ82, which blocks the ATP binding pocket, or CW069, which binds to an allosteric site. However, cells with a normal complement of centrosomes are still affected by these inhibitors and, whilst only transient, multipolarity can occur in these cells that may either trigger cell death or induce genetic instability.

One concern with certain compounds developed as centrosome de-clustering agents, such as griseofulvin and its derivatives (43), is that they induce formation of acentrosomal spindle poles, i.e. poles that do not contain or arise from bona fide centrosomes. Similar acentrosomal poles are formed upon treatment of cells with taxol-based drugs, and this could be a common feature of de-clustering agents that work by disturbing microtubule dynamics or motors that crosslink microtubules. The fact that we never saw acentrosomal poles upon loss of Hsp72 or Nek6 function argues that this pathway acts through some other mechanism. The fluorescent tubulin probe allowed us to directly monitor microtubule organization in live mitotic cells and revealed that it is resolution of a multipolar to bipolar state that is inhibited in cells with amplified centrosomes. This was supported by nocodazole washout experiments that showed acentrosomal poles formed in HeLa cells with normal centrosome numbers clustered efficiently in the presence of the Hsp70 inhibitor. These data rather argue for a specific role for this pathway at points of microtubule attachment to centrosomes, kinetochores or the cell cortex and is reassuring from a therapeutic perspective as it demonstrates selectivity towards cells with amplified centrosomes.

There is further potential patient-benefit in targeting the Nek6-Hsp72 pathway as both components are overexpressed in cancer versus normal cells (50,51). Moreover, normal cells may have a reduced requirement for this pathway compared to cancer cells with no evidence of mitotic delays or segregation errors in either immortalised RPE1 or HBL100 cells. From a practical perspective though there are limitations in directly targeting Hsp72. First, different Hsp70 family members are highly similar in active site structure and it will be difficult to develop catalytic inhibitors that don't also target other family members with essential roles in normal cell homeostasis. For this reason, simply measuring cell survival in response to Hsp70 inhibition may well not reveal a direct correlation with centrosome number. Second, Hsp70 is proving to be a challenging drug target due to its high affinity for nucleotide. In contrast, having demonstrated a requirement for Nek6 activity for centrosome clustering, this kinase may well make a more attractive target than Hsp72. Indeed, while there is significant sequence similarity within the catalytic sites with other NEKs, particularly Nek7, we are developing approaches to generate

selective inhibitors that target not only the catalytic site but also the more divergent allosteric sites required for activation (52).

At the same time as developing Nek6 inhibitors, we need to identify groups of patients who might benefit from centrosome de-clustering agents. Although inhibiting this pathway causes problems in mitotic progression in cancer cells even without centrosome amplification, we argue that extra centrosomes would sensitise cancer cells to mitotic catastrophe in a physiological setting and are therefore a valuable and relatively easy to measure biomarker, especially in haematological malignancies (4). Genetic changes known to cause centrosome amplification, such as Aurora-A overexpression or BRCA1 loss, may also represent useful biomarkers for selecting clinical trial cohorts (8). Here, we show that a subset of ALL cell lines harbour amplified centrosomes and most of these have the capacity to cluster the extra centrosomes to avoid generating multipolar spindles. Furthermore, treatment with an Hsp70 inhibitor led to loss of clustering with the frequency of multipolar spindles closely reflecting the extent of centrosome amplification. ALL cells represent a good model for a disease that has traditionally been treated with anti-mitotic chemotherapies and, although we haven't explored cell survival for the reasons given above, it could be that centrosome number acts as a biomarker for stratification. High levels of centrosome amplification have previously been observed in other haematological malignancies, including DLBCL, MCL and CML (4). Future work will be important to identify genetic signatures that dictate the response of blood cancers to centrosome de-clustering strategies and enable the clinical development of new targeted agents.

ACKNOWLEDGMENTS

We thank Dr Sandrine Jayne and Dr Ildiko Gyory (Leicester) for assistance with ALL cell culture. We acknowledge support of the Advanced Imaging Facility of the University of Leicester Core Biotechnology Services.

REFERENCES

1. Heald R, Khodjakov A. Thirty years of search and capture: The complex simplicity of mitotic spindle assembly. J Cell Biol 2015;211(6):1103-11.
2. Walczak CE, Heald R. Mechanisms of mitotic spindle assembly and function. International review of cytology 2008;265:111-58.
3. Chan JY. A clinical overview of centrosome amplification in human cancers. International journal of biological sciences 2011;7(8):1122-44.
4. Kramer A, Neben K, Ho AD. Centrosome aberrations in hematological malignancies. Cell Biol Int 2005;29(5):375-83.
5. Ganem NJ, Godinho SA, Pellman D. A mechanism linking extra centrosomes to chromosomal instability. Nature 2009;460(7252):278-82.
6. Thompson SL, Compton DA. Chromosome missegregation in human cells arises through specific types of kinetochore-microtubule attachment errors. Proc Natl Acad Sci U S A 2011;108(44):17974-8.
7. Silkworth WT, Nardi IK, Scholl LM, Cimini D. Multipolar spindle pole coalescence is a major source of kinetochore mis-attachment and chromosome mis-segregation in cancer cells. PloS one 2009;4(8):e6564.
8. Gordon DJ, Resio B, Pellman D. Causes and consequences of aneuploidy in cancer. Nat Rev Genet 2012;13(3):189-203.
9. Vitre BD, Cleveland DW. Centrosomes, chromosome instability (CIN) and aneuploidy. Curr Opin Cell Biol 2012;24(6):809-15.
10. Thompson SL, Bakhoum SF, Compton DA. Mechanisms of chromosomal instability. Curr Biol 2010;20(6):R285-95.
11. Nigg EA, Stearns T. The centrosome cycle: Centriole biogenesis, duplication and inherent asymmetries. Nat Cell Biol 2011;13(10):1154-60.
12. Conduit PT, Wainman A, Raff JW. Centrosome function and assembly in animal cells. Nat Rev Mol Cell Biol 2015;16(10):611-24.
13. Mennella V, Agard DA, Huang B, Pelletier L. Amorphous no more: subdiffraction view of the pericentriolar material architecture. Trends Cell Biol 2014;24(3):188-97.
14. Brito DA, Gouveia SM, Bettencourt-Dias M. Deconstructing the centriole: structure and number control. Curr Opin Cell Biol 2012;24(1):4-13.
15. Mardin BR, Schiebel E. Breaking the ties that bind: new advances in centrosome biology. J Cell Biol 2012;197(1):11-8.
16. Leber B, Maier B, Fuchs F, Chi J, Riffel P, Anderhub S, et al. Proteins required for centrosome clustering in cancer cells. Science translational medicine 2010;2(33):33ra38.
17. Quintyne NJ, Reing JE, Hoffelder DR, Gollin SM, Saunders WS. Spindle multipolarity is prevented by centrosomal clustering. Science 2005;307(5706):127-9.

18. Kwon M, Godinho SA, Chandhok NS, Ganem NJ, Azioune A, Thery M, et al. Mechanisms to suppress multipolar divisions in cancer cells with extra centrosomes. Genes & development 2008;22(16):2189-203.
19. Drosopoulos K, Tang C, Chao WC, Linardopoulos S. APC/C is an essential regulator of centrosome clustering. Nat Commun 2014;5:3686.
20. Ogden A, Rida PC, Aneja R. Let's huddle to prevent a muddle: centrosome declustering as an attractive anticancer strategy. Cell death and differentiation 2012;19(8):1255-67.
21. Godinho SA, Pellman D. Causes and consequences of centrosome abnormalities in cancer. Philos Trans R Soc Lond B Biol Sci 2014;369(1650).
22. Fukasawa K. Oncogenes and tumour suppressors take on centrosomes. Nat Rev Cancer 2007;7(12):911-24.
23. Orr B, Compton DA. A double-edged sword: how oncogenes and tumor suppressor genes can contribute to chromosomal instability. Front Oncol 2013;3:164.
24. Ganem NJ, Cornils H, Chiu SY, O'Rourke KP, Arnaud J, Yimlamai D, et al. Cytokinesis failure triggers hippo tumor suppressor pathway activation. Cell 2014;158(4):833-48.
25. Hartl FU, Bracher A, Hayer-Hartl M. Molecular chaperones in protein folding and proteostasis. Nature 2011;475(7356):324-32.
26. Bukau B, Weissman J, Horwich A. Molecular chaperones and protein quality control. Cell 2006;125(3):443-51.
27. Luo J, Solimini NL, Elledge SJ. Principles of cancer therapy: oncogene and non-oncogene addiction. Cell 2009;136(5):823-37.
28. Hanahan D, Weinberg RA. Hallmarks of cancer: the next generation. Cell 2011;144(5):646-74.
29. O'Regan L, Sampson J, Richards MW, Knebel A, Roth D, Hood FE, et al. Hsp72 is targeted to the mitotic spindle by Nek6 to promote K-fiber assembly and mitotic progression. J Cell Biol 2015;209(3):349-58.
30. Fielding AB, Lim S, Montgomery K, Dobreva I, Dedhar S. A critical role of integrin-linked kinase, ch-TOG and TACC3 in centrosome clustering in cancer cells. Oncogene 2011;30(5):521-34.
31. Pannu V, Rida PC, Celik B, Turaga RC, Ogden A, Cantuaria G, et al. Centrosome-declustering drugs mediate a two-pronged attack on interphase and mitosis in supercentrosomal cancer cells. Cell Death Dis 2014;5:e1538.
32. O'Regan L, Fry AM. The Nek6 and Nek7 protein kinases are required for robust mitotic spindle formation and cytokinesis. Mol Cell Biol 2009;29(14):3975-90.
33. Sampson J, Fry AM. Monitoring centrosome clustering in cancer cells. In: Dawe H, editor. The centriole: methods and protocols. Volume in press, Methods in Molcular Biology: Springer; 2016.

34. Hames RS, Crookes RE, Straatman KR, Merdes A, Hayes MJ, Faragher AJ, et al. Dynamic recruitment of Nek2 kinase to the centrosome involves microtubules, PCM-1, and localized proteasomal degradation. Mol Biol Cell 2005;16(4):1711-24.
35. Massey AJ, Williamson DS, Browne H, Murray JB, Dokurno P, Shaw T, et al. A novel, small molecule inhibitor of Hsc70/Hsp70 potentiates Hsp90 inhibitor induced apoptosis in HCT116 colon carcinoma cells. Cancer chemotherapy and pharmacology 2010;66(3):535-45.
36. Lukinavicius G, Reymond L, D'Este E, Masharina A, Gottfert F, Ta H, et al. Fluorogenic probes for live-cell imaging of the cytoskeleton. Nat Methods 2014;11(7):731-3.
37. de Souza EE, Meirelles GV, Godoy BB, Perez AM, Smetana JH, Doxsey SJ, et al. Characterization of the human Nek7 interactome suggests catalytic and regulatory properties distinct from Nek6. Journal of proteome research 2014;13:4074-90.
38. Geraci F, Agueli C, Giudice G, Sconzo G. Localization of HSP70, Cdc2, and cyclin B in sea urchin oocytes in non-stressed conditions. Biochemical and biophysical research communications 2003;310(3):748-53.
39. Agueli C, Geraci F, Giudice G, Chimenti L, Cascino D, Sconzo G. A constitutive 70 kDa heat-shock protein is localized on the fibres of spindles and asters at metaphase in an ATP-dependent manner: a new chaperone role is proposed. The Biochemical journal 2001;360(Pt 2):413-9.
40. Hut HM, Kampinga HH, Sibon OC. Hsp70 protects mitotic cells against heat-induced centrosome damage and division abnormalities. Mol Biol Cell 2005;16(8):3776-85.
41. Sdelci S, Bertran MT, Roig J. Nek9, Nek6, Nek7 and the separation of centrosomes. Cell Cycle 2011;10(22):3816-7.
42. Bertran MT, Sdelci S, Regue L, Avruch J, Caelles C, Roig J. Nek9 is a Plk1-activated kinase that controls early centrosome separation through Nek6/7 and Eg5. EMBO J 2011;30(13):2634-47.
43. Rebacz B, Larsen TO, Clausen MH, Ronnest MH, Loffler H, Ho AD, et al. Identification of griseofulvin as an inhibitor of centrosomal clustering in a phenotype-based screen. Cancer research 2007;67(13):6342-50.
44. Goldberg JM, Silverman LB, Levy DE, Dalton VK, Gelber RD, Lehmann L, et al. Childhood T-cell acute lymphoblastic leukemia: the Dana-Farber Cancer Institute acute lymphoblastic leukemia consortium experience. J Clin Oncol 2003;21(19):3616-22.
45. Basto R, Brunk K, Vinadogrova T, Peel N, Franz A, Khodjakov A, et al. Centrosome amplification can initiate tumorigenesis in flies. Cell 2008;133(6):1032-42.
46. Clerico EM, Tilitsky JM, Meng W, Gierasch LM. How hsp70 molecular machines interact with their substrates to mediate diverse physiological functions. J Mol Biol 2015;427(7):1575-88.

47. Hood FE, Williams SJ, Burgess SG, Richards MW, Roth D, Straube A, et al. Coordination of adjacent domains mediates TACC3-ch-TOG-clathrin assembly and mitotic spindle binding. J Cell Biol 2013;202(3):463-78.
48. Wu J, Mikule K, Wang W, Su N, Petteruti P, Gharahdaghi F, et al. Discovery and mechanistic study of a small molecule inhibitor for motor protein KIFC1. ACS Chem Biol 2013;8(10):2201-8.
49. Watts CA, Richards FM, Bender A, Bond PJ, Korb O, Kern O, et al. Design, synthesis, and biological evaluation of an allosteric inhibitor of HSET that targets cancer cells with supernumerary centrosomes. Chem Biol 2013;20(11):1399-410.
50. Nassirpour R, Shao L, Flanagan P, Abrams T, Jallal B, Smeal T, et al. Nek6 mediates human cancer cell transformation and is a potential cancer therapeutic target. Mol Cancer Res 2010;8(5):717-28.
51. Powers MV, Jones K, Barillari C, Westwood I, van Montfort RL, Workman P. Targeting HSP70: The second potentially druggable heat shock protein and molecular chaperone? Cell Cycle 2010;9(8):1542-50.
52. Haq T, Richards MW, Burgess SG, Gallego P, Yeoh S, O'Regan L, et al. Mechanistic basis of Nek7 activation through Nek9 binding and induced dimerization. Nat Commun 2015;6:8771.

FIGURE LEGENDS

Figure 1. Loss of Hsp72 function blocks centrosome clustering

A. MDA-MB-231, HeLa, NIE-115 and RPE1 cells were stained for centrin-2 (green), γ-tubulin (red) and DNA (blue). **B.** Histogram shows the percentage of interphase cells from A exhibiting centrosome amplification (CA, >2 centrosomes). **C.** MDA-MB-231 and NIE-115 cells were stained for centrin-2 (green), α-tubulin (red) and DNA (blue). **D.** Histogram shows the percentage of metaphase cells from C with amplified centrosomes with bipolar or multipolar spindles. **E.** MDA-MB-231 and NIE-115 cells were either untreated (control) or treated with the Hsp70i at the dose indicated before being fixed and stained as in C. **F, G.** Histograms show the percentage of cells with amplified centrosomes shown in E that had multipolar spindles. **H. I**. Histograms show the percentage of cells with amplified centrosomes that had multipolar spindles following mock or Hsp72 depletion using two distinct siRNAs. In A, C and E, scale bars, 5 μm; magnified views of centrosomes are shown. Data in B, D, F, G, H and I are n=4, >400 cells.

Figure 2. Resolution of a multipolar to bipolar state is blocked by Hsp70 inhibition

A. NIE-115 cells were incubated with SiR-tubulin prior to time-lapse imaging in the presence or absence of Hsp70i. Still images are shown of SiR-tubulin alone (top rows) and merged with brightfield (BF; bottom rows) at the times indicated. Arrowheads indicate spindle poles; arrows indicate daughter cells following division. Scale bars, 20 μm. **B.** Time-lapse imaging of NIE-115 cells in the absence (control) or presence of Hsp70i was used to determine the time spent in each stage of mitosis as indicated; each bar is representative of a single cell. **C, D.** Histograms show the time spent with a multipolar spindle in control, Hsp70i treated or siHsp72-depleted NIE-115 (C) or MDA-MB-231 (D) cells; n=3; 15 cells.

Figure 3. Nek6 kinase activity is required for centrosome clustering

A. MDA-MB-231 cells were mock-depleted or depleted with siRNAs against Nek6 or Nek7 before being stained for centrin-2 (green) and α-tubulin (red). Merge images include DNA (blue). **B.**

Histogram shows the percentage of mitotic cells with amplified centrosomes that had multipolar spindles. Cells were treated as in A, as well as transfected with wild-type or kinase-dead (KD) Flag-Nek6 following Nek6 depletion. The different Nek6 and Nek7 siRNAs used are indicated. **C**. MDA-MB-231 cells that were mock-depleted, depleted of Nek6 or Nek7, or treated with Aurora-A or PLK1 inhibitors were stained for Hsp72 (green), α-tubulin (red) and DNA (blue in merge). **D.** Histogram shows the spindle intensity of Hsp72 relative to microtubules in mitotic MDA-MB-231 cells treated as indicated. Data in B and D, n=3, >300 cells. **E**. NIE-115 cells that were mock-treated or treated with Aurora-A or PLK1 inhibitors were stained for Hsp72 (green), α-tubulin (red) and DNA (blue in merge). Scale bars in A, C and E, 5 μm.

Figure 4. Loss of Hsp72 or Nek6 function does not induce acentrosomal pole formation

A. MDA-MB-231 and HeLa cells were either untreated (control) or treated with 10 μM griseofulvin before being stained for centrin-2 (green). Merge panels include α-tubulin (red) and DNA (blue). **B.** Histogram shows the percentage of cells with amplified centrosomes that had multipolar spindles following the treatments shown. **C.** MDA-MB-231 cells that were depleted with siRNAs against Hsp72 or Nek6 as indicated, or treated with 10 μM griseofulvin, were stained as in A. **D.** Histogram shows the percentage of mitotic MDA-MB-231 cells from C, as well as HeLa cells treated with 10 μM griseofulvin, with acentrosomal spindle poles. **E-G.** The percentage of mitotic NIE-115 (E), MDA-MB-231 (F) and HeLa (G) cells with >2 microtubule asters upon release into nocodazole-free media in the absence (control, black line) or presence (red line) of Hsp70i is indicated. Enlarged views of spindle poles are shown in A and C; scale bars, 5 μm. Data in B and D-G, n=3, >200 cells.

Figure 5. Hsp70 inhibition blocks centrosome clustering in ALL cells

A. Peripheral blood lymphocyte (PBL) or acute lymphoblastic leukaemia (ALL) cell lines were stained for CEP135, γ-tubulin and DNA. Enlargements of centrosomes are shown. **B.** Histogram shows percentage of interphase cells with amplified centrosomes. **C.** Cells were treated with 10 μM Hsp70i for 4 h and stained for CEP135, α-tubulin and DNA. **D.** Histogram shows the

percentage of mitotic cells with multipolar spindles following Hsp70i treatment at the dose indicated (μM). **E.** Cells were treated with 10 μM griseofulvin and stained for pericentrin, α-tubulin and DNA. **F.** Histogram shows percentage of mitotic cells with multipolar spindles following griseofulvin treatment at the dose indicated (μM). Scale bars in A, C and E, 2.5 μm. Data in B, D and F, n=4, >400 cells.

Figure 6. Hsp70 inhibition does not interfere with mitosis in diploid cells

A. Cells that were untreated (control, MDA-MB-231) or treated with 10 μM Hsp70i for 4 h were stained with CenpA (green) and α-tubulin (red). Misaligned chromosomes are indicated with arrowheads. **B.** Histogram shows the percentage of mitotic cells with misaligned chromosomes upon treatment with Hsp70i at the dose indicated. **C.** Histogram shows the percentage of mitotic cells with misaligned chromosomes following mock depletion or depletion of Hsp72 or Nek6 as indicated. **D.** Histogram shows the mitotic index upon Hsp70i treatment at the dose indicated. Data in B-D, n=4, >400 cells. **E.** Time-lapse imaging of RPE1 cells was performed in the presence of SiR-tubulin following no treatment, 10 μM Hsp70i or Hsp72 depletion and the duration of mitosis recorded for 20 cells in each condition; each dot represents one cell. **F**. MDA-MB-231 cells were treated with nocodazole for 16 hours before further addition of DMSO or Hsp70i for 4 hours. Cells were stained with BubR1 (green). Merge images in A and F include DNA (blue); scale bars, 5 μm. **G**. Histogram of BubR1 intensity at kinetochores relative to CenpA. **H**. The schematic model shows the Nek6-Hsp72 pathway (including upstream activators) promoting centrosome (red dots) clustering and pseudo-bipolar spindle formation, with declustering and multipolarity resulting from Hsp70 inhibition, or depletion of Hsp72 or Nek6.

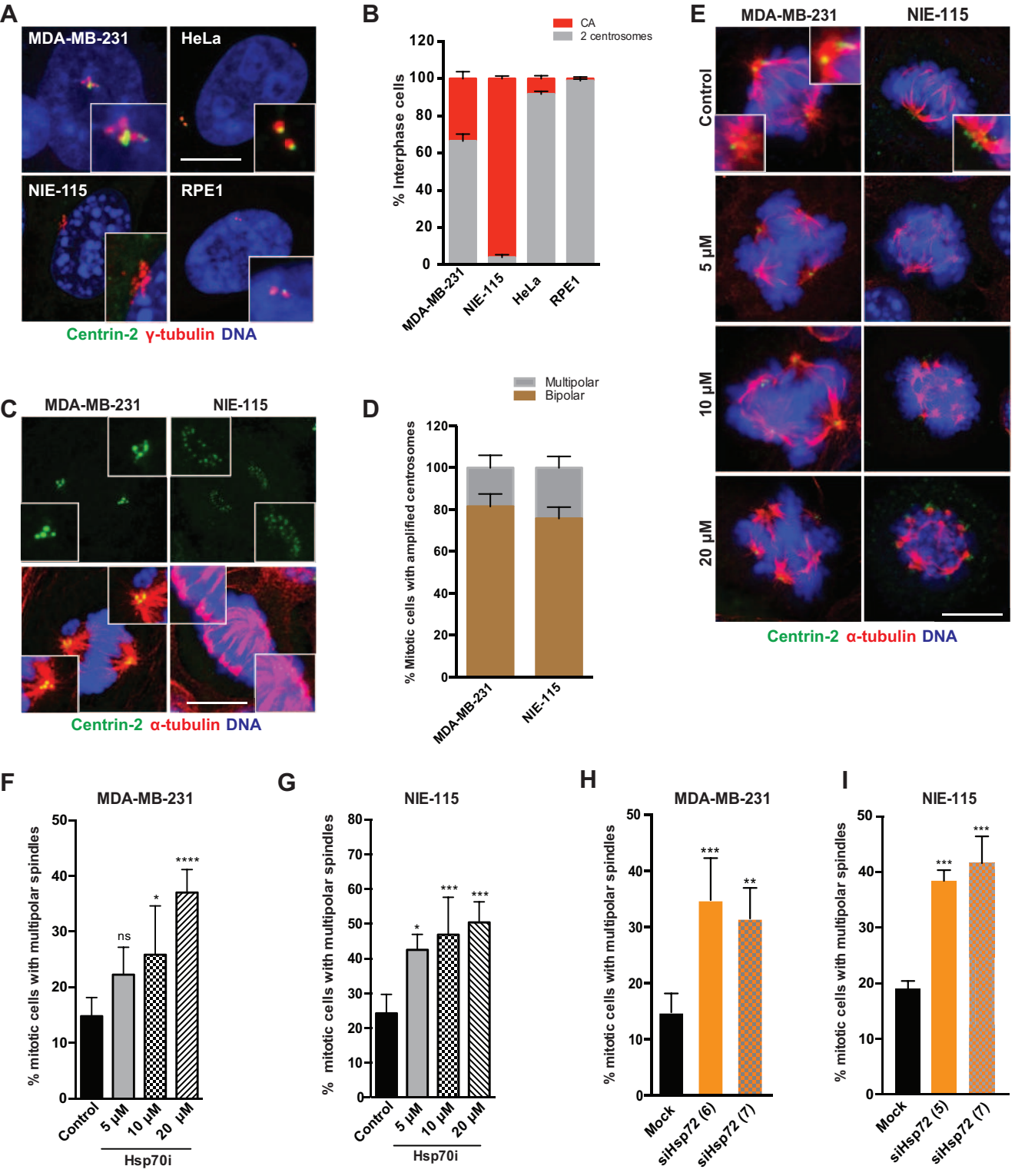
A
MDA-MB-231
HeLa
NIE-115
RPE1
Centrin-2 γ-tubulin DNA
B
CA
2 centrosomes
% Interphase cells
120
100
80
60
40
20
0
MDA-MB-231
NIE-115
HeLa
RPE1
C
MDA-MB-231
NIE-115
Centrin-2 α-tubulin DNA
D
Multipolar
Bipolar
% Mitotic cells with amplified centrosomes
120
100
80
60
40
20
0
MDA-MB-231
NIE-115
E
MDA-MB-231
NIE-115
Control
5 μM
10 μM
20 μM
Centrin-2 α-tubulin DNA
F
MDA-MB-231
% mitotic cells with multipolar spindles
50
40
30
20
10
0
ns
*
****
Control
5 μM
10 μM
20 μM
Hsp70i
G
NIE-115
% mitotic cells with multipolar spindles
80
70
60
50
40
30
20
10
0
*
***
***
Control
5 μM
10 μM
20 μM
Hsp70i
H
MDA-MB-231
% mitotic cells with multipolar spindles
50
40
30
20
10
0
***
**
Mock
siHsp72 (6)
siHsp72 (7)
I
NIE-115
% mitotic cells with multipolar spindles
50
40
30
20
10
0
***
***
Mock
siHsp72 (5)
siHsp72 (7)

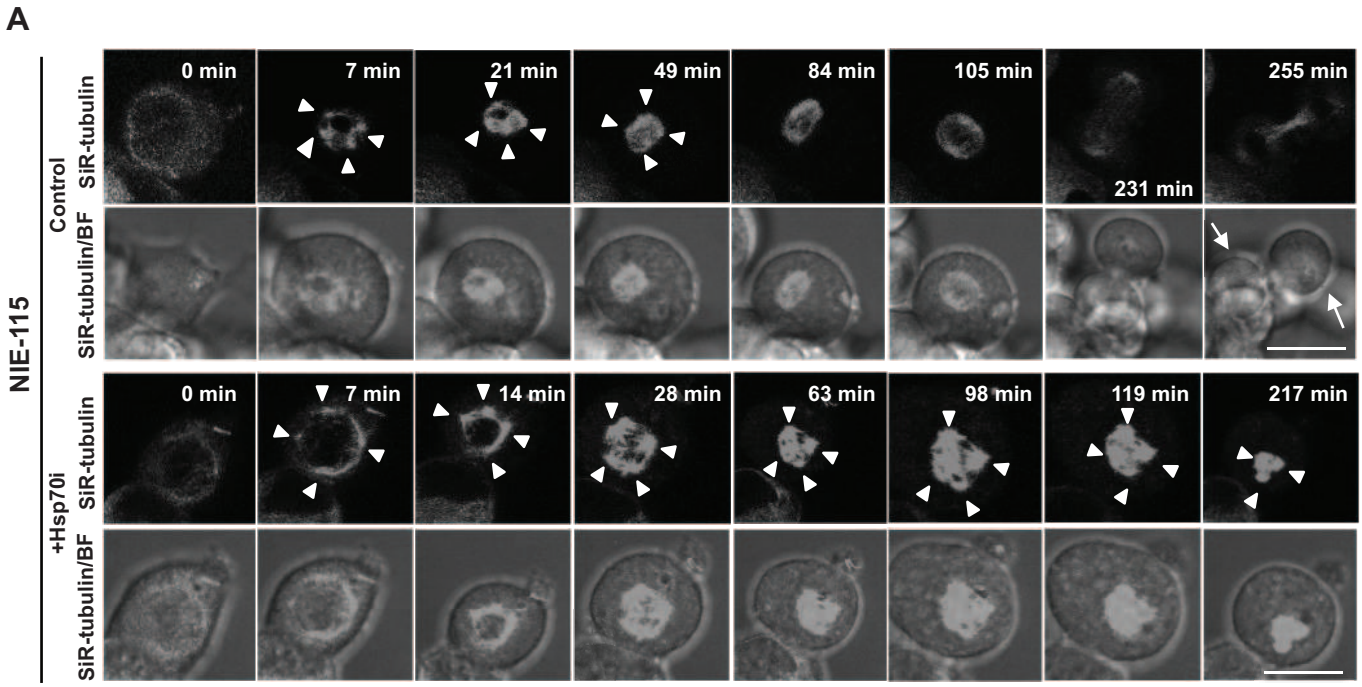
A
NIE-115
Control
SiR-tubulin
SiR-tubulin/BF
+Hsp70i
SiR-tubulin
SiR-tubulin/BF
0 min
7 min
21 min
49 min
84 min
105 min
231 min
255 min
0 min
7 min
14 min
28 min
63 min
98 min
119 min
217 min

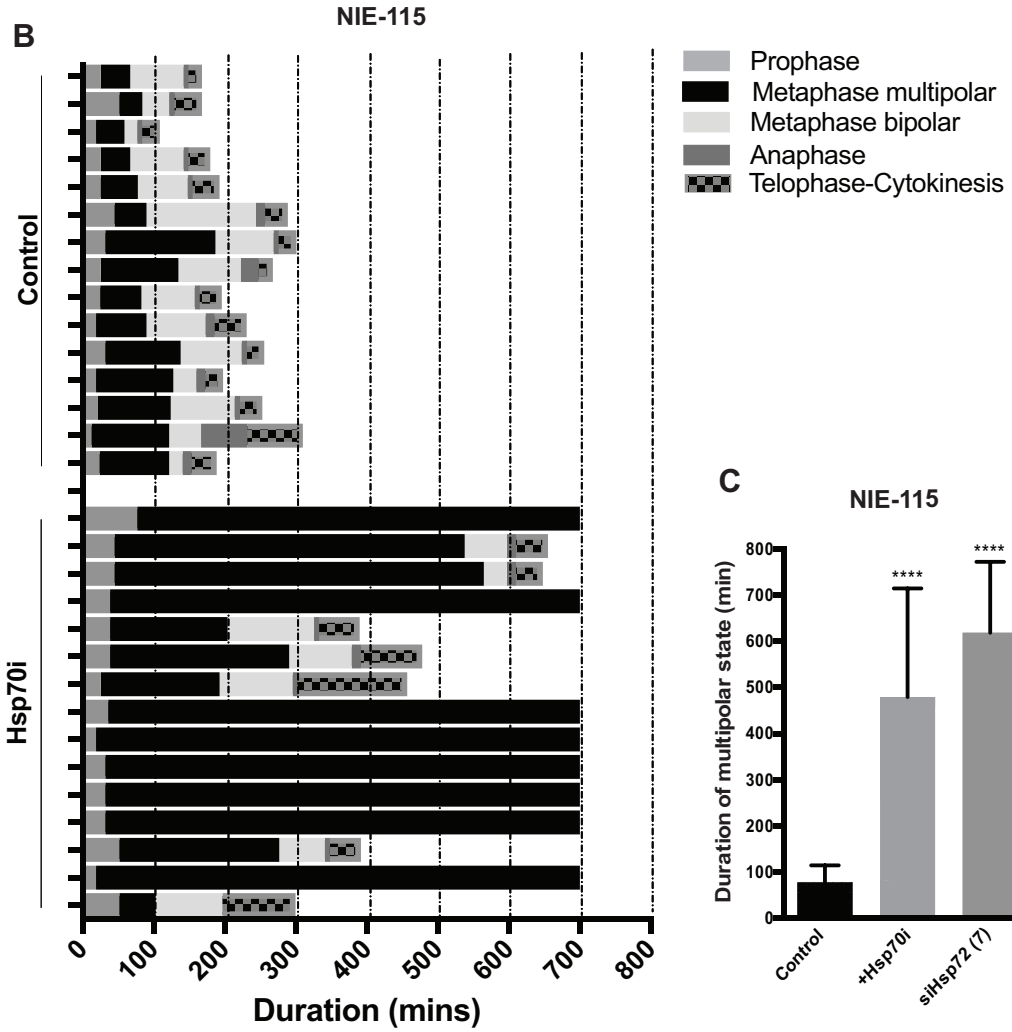
B
NIE-115
Control
Hsp70i
Prophase
Metaphase multipolar
Metaphase bipolar
Anaphase
Telophase-Cytokinesis
0
100
200
300
400
500
600
700
800
Duration (mins)

C
NIE-115
Duration of multipolar state (min)
0
100
200
300
400
500
600
700
800
****
****
Control
+Hsp70i
siHsp72 (7)

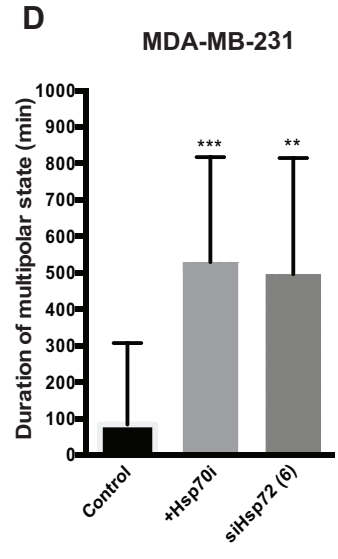
D
MDA-MB-231
Duration of multipolar state (min)
0
100
200
300
400
500
600
700
800
900
1000
***
**
Control
+Hsp70i
siHsp72 (6)

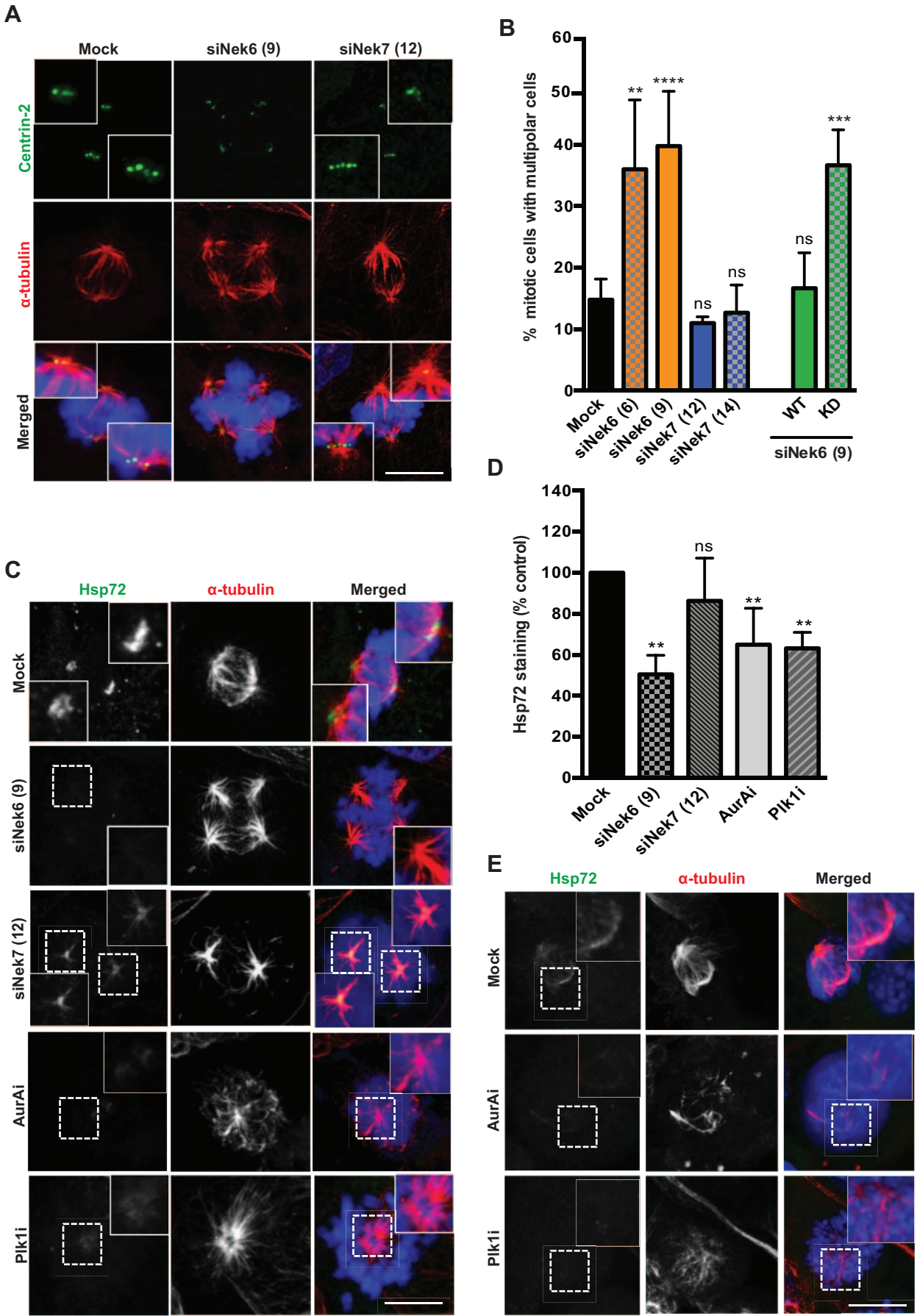
A
Mock
siNek6 (9)
siNek7 (12)
Centrin-2
α-tubulin
Merged
B
% mitotic cells with multipolar cells
60
50
40
30
20
10
0
**
****
ns
ns
ns
***
Mock
siNek6 (6)
siNek6 (9)
siNek7 (12)
siNek7 (14)
WT
KD
siNek6 (9)
C
Hsp72
α-tubulin
Merged
Mock
siNek6 (9)
siNek7 (12)
AurAi
Plk1i
D
Hsp72 staining (% control)
140
120
100
80
60
40
20
0
**
ns
**
**
Mock
siNek6 (9)
siNek7 (12)
AurAi
Plk1i
E
Hsp72
α-tubulin
Merged
Mock
AurAi
Plk1i

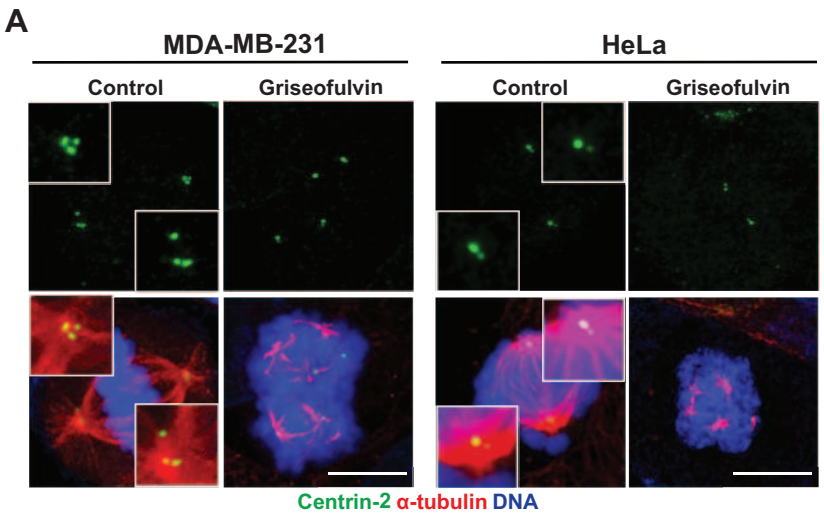
A
MDA-MB-231
HeLa
Control
Griseofulvin
Control
Griseofulvin
Centrin-2 α-tubulin DNA

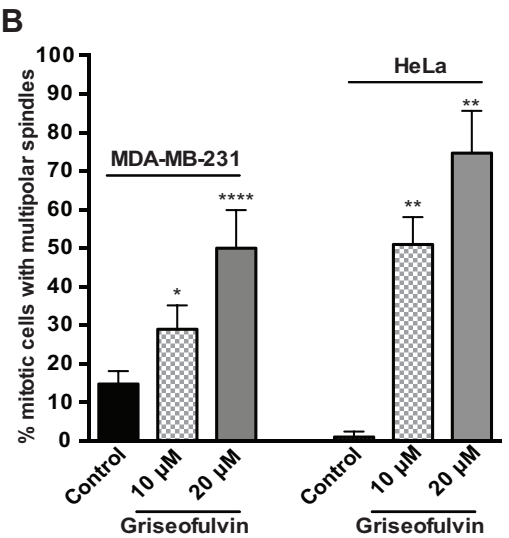
B
% mitotic cells with multipolar spindles
HeLa
MDA-MB-231
Control
10 μM
20 μM
Griseofulvin

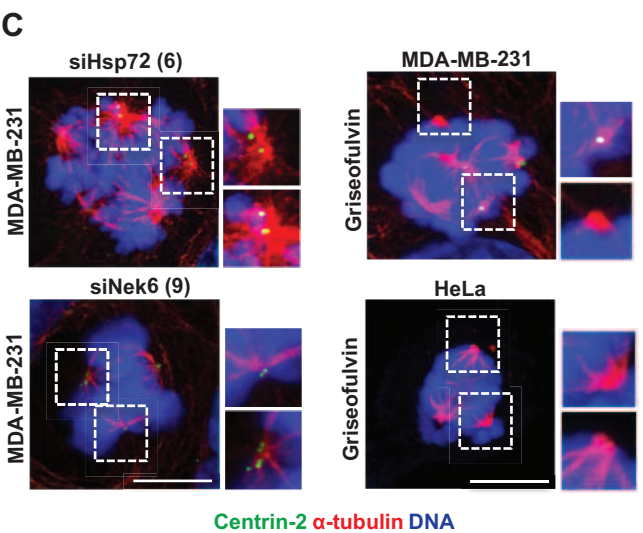
C
siHsp72 (6)
MDA-MB-231
Griseofulvin
siNek6 (9)
HeLa
Centrin-2 α-tubulin DNA

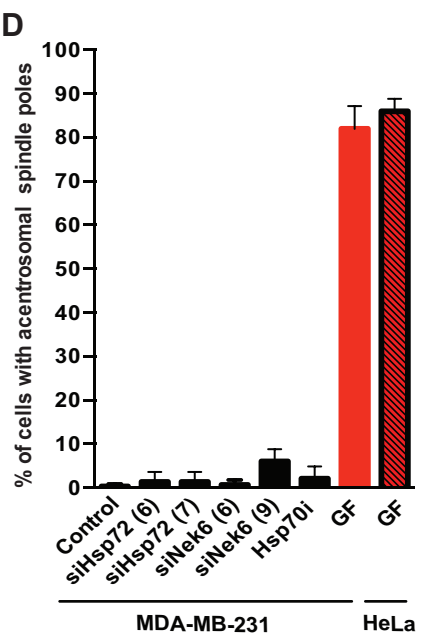
D
% of cells with acentrosomal spindle poles
Control
siHsp72 (6)
siHsp72 (7)
siNek6 (6)
siNek6 (9)
Hsp70i
GF
GF
MDA-MB-231
HeLa

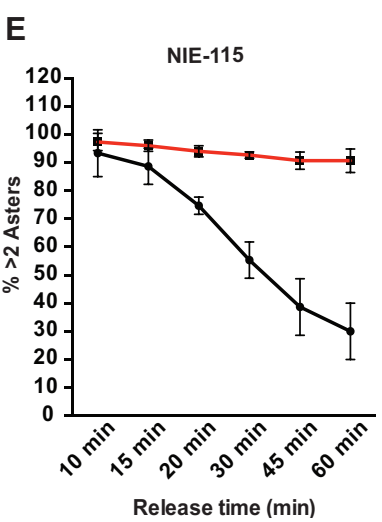
E
NIE-115
% >2 Asters
10 min
15 min
20 min
30 min
45 min
60 min
Release time (min)

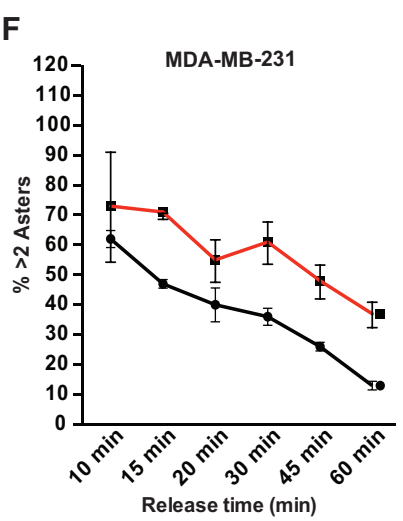
F
MDA-MB-231
% >2 Asters
10 min
15 min
20 min
30 min
45 min
60 min
Release time (min)

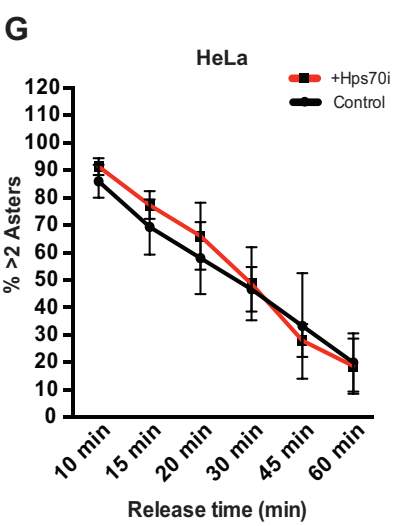
G
HeLa
+Hps70i
Control
% >2 Asters
10 min
15 min
20 min
30 min
45 min
60 min
Release time (min)

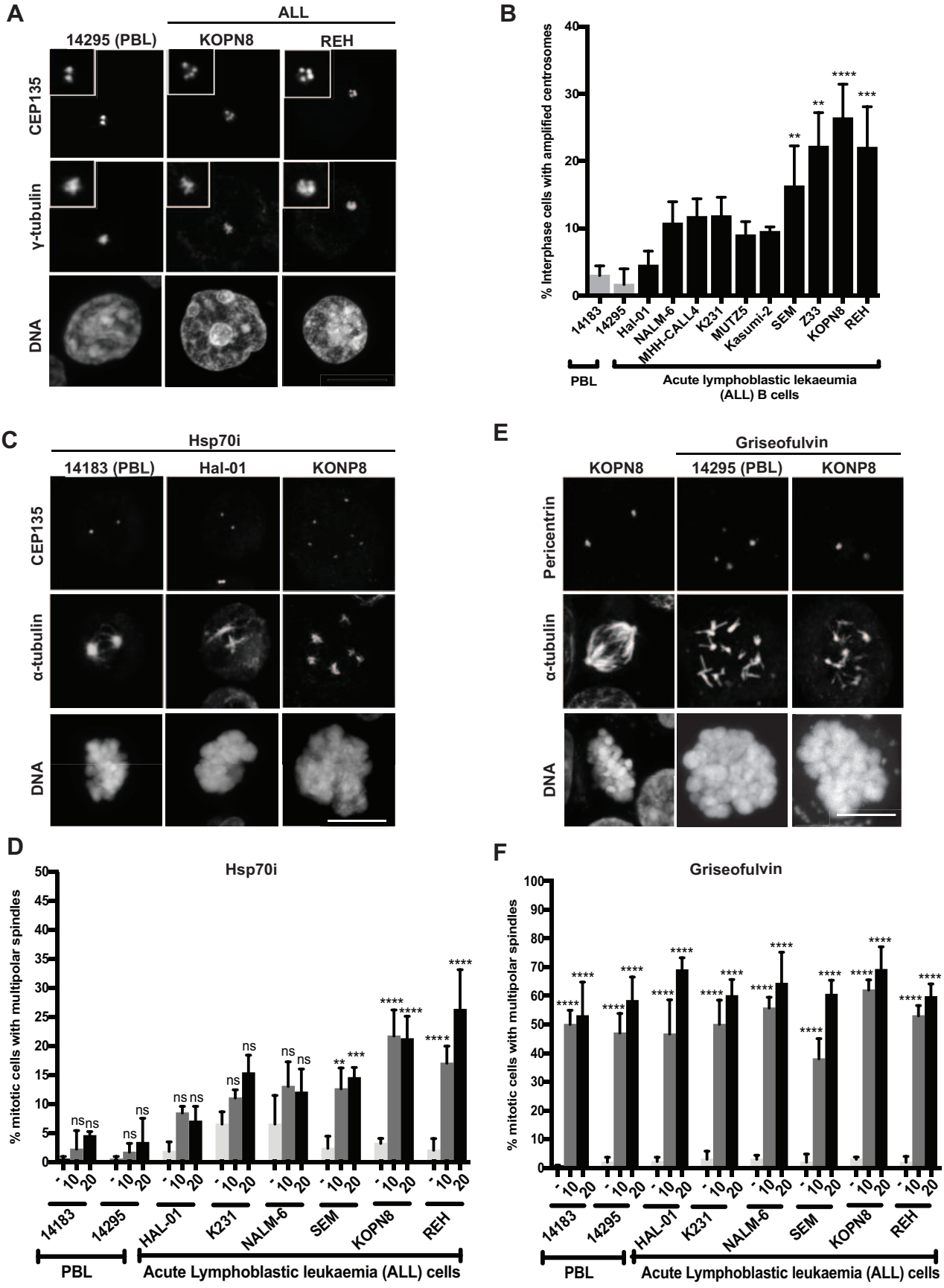
A
ALL
14295 (PBL)
KOPN8
REH
CEP135
γ-tubulin
DNA
B
% Interphase cells with amplified centrosomes
14183
14295
Hal-01
NALM-6
MHH-CALL4
K231
MUTZ5
Kasumi-2
SEM
Z33
KOPN8
REH
PBL
Acute lymphoblastic lekaeumia (ALL) B cells
C
Hsp70i
14183 (PBL)
Hal-01
KONP8
CEP135
α-tubulin
DNA
D
Hsp70i
% mitotic cells with multipolar spindles
PBL
Acute Lymphoblastic leukaemia (ALL) cells
E
Griseofulvin
KOPN8
14295 (PBL)
KONP8
Pericentrin
α-tubulin
DNA
F
Griseofulvin
% mitotic cells with multipolar spindles
PBL
Acute Lymphoblastic leukaemia (ALL) cells

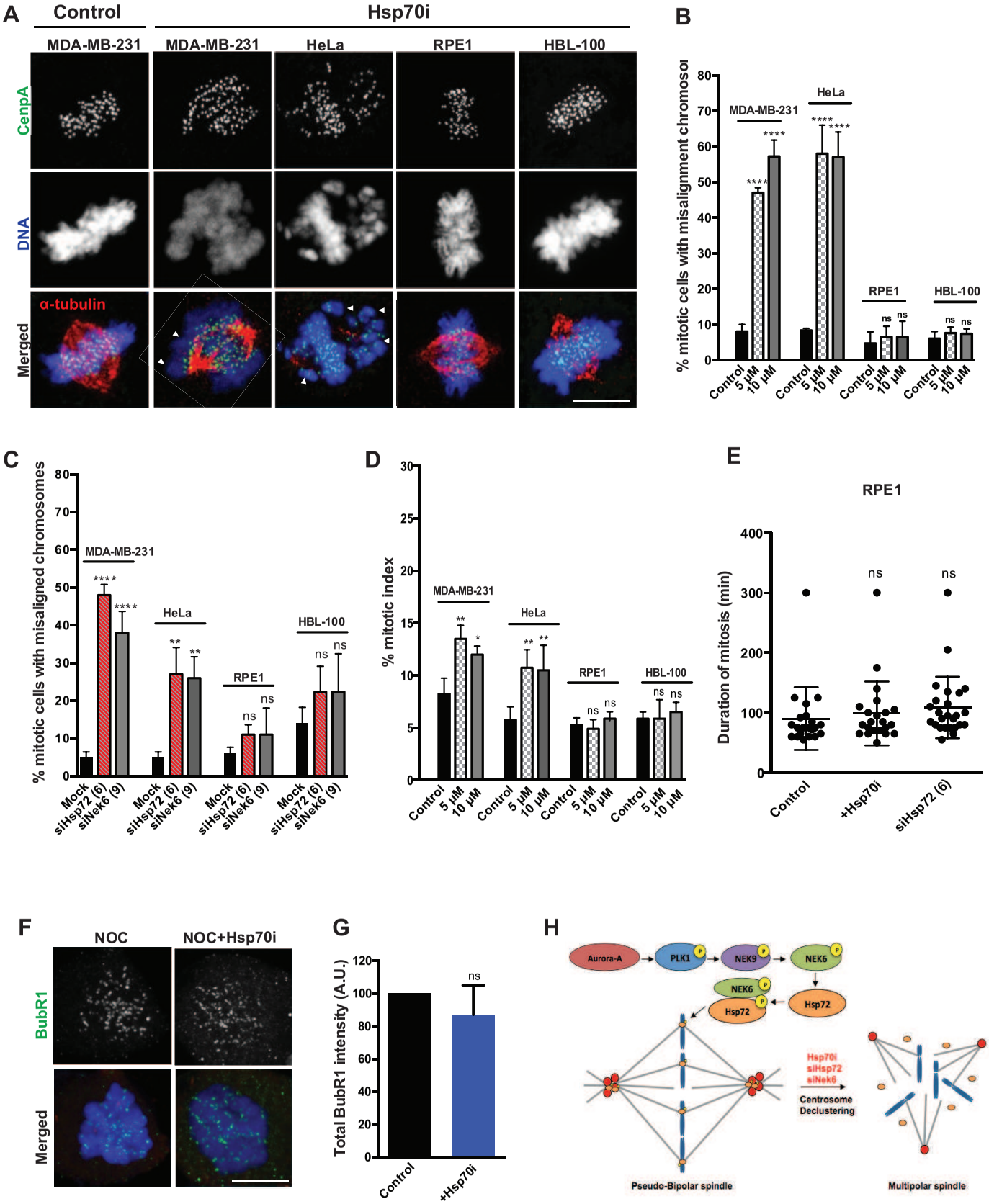
A
Control
Hsp70i
MDA-MB-231
MDA-MB-231
HeLa
RPE1
HBL-100
CenpA
DNA
α-tubulin
Merged
B
% mitotic cells with misalignment chromosoi
MDA-MB-231
HeLa
RPE1
HBL-100
Control
5 μM
10 μM
C
% mitotic cells with misaligned chromosomes
MDA-MB-231
HeLa
RPE1
HBL-100
Mock
siHsp72 (6)
siNek6 (9)
D
% mitotic index
MDA-MB-231
HeLa
RPE1
HBL-100
Control
5 μM
10 μM
E
RPE1
Duration of mitosis (min)
Control
+Hsp70i
siHsp72 (6)
F
NOC
NOC+Hsp70i
BubR1
Merged
G
Total BubR1 intensity (A.U.)
Control
+Hsp70i
H
Aurora-A
PLK1
NEK9
NEK6
Hsp72
Hsp70i
siHsp72
siNek6
Centrosome Declustering
Pseudo-Bipolar spindle
Multipolar spindle